Synergetic Effect of Potassium Persulfate and Iron Oxalate on Photodegradation of Para-Arsanilic Acid

Yuliya E. Tyutereva
Voevodsky Institute of Chemical Kinetics and Combustion SB RAS: Institut himiceskoj kinetiki i gorenia imeni V V Voevodskogo SO RAN

Petr S. Sherin
International Tomography Center SB RAS: Mezdunarodnyj tomograficeskij centr SO RAN

Evgeniya V. Polyakova
Nikolaev Institute of Inorganic Chemistry: Institut neorganiceskoj himii imeni A V Nikolaeva

Vyacheslav P. Grivin
Voevodsky Institute of Chemical Kinetics and Combustion SB RAS: Institut himiceskoj kinetiki i gorenia imeni V V Voevodskogo SO RAN

Victor F. Plyusnin
Voevodsky Institute of Chemical Kinetics and Combustion SB RAS: Institut himiceskoj kinetiki i gorenia imeni V V Voevodskogo SO RAN

Olga V. Shuvaeva
Nikolaev Institute of Inorganic Chemistry: Institut neorganiceskoj himii imeni A V Nikolaeva

Jing Xu
Wuhan University

Feng Wu
Wuhan University

Ivan P. Pozdnyakov (ipozdnyak@kinetics.nsc.ru)
Voevodsky Institute of Chemical Kinetics and Combustion SB RAS: Institut himiceskoj kinetiki i gorenia imeni V V Voevodskogo SO RAN https://orcid.org/0000-0003-3320-9567

Research Article

Keywords: ferrioxalate complex, p-ASA, AOPs, hydroxyl radical, sulfate radical, photodegradation, laser flash photolysis

Posted Date: May 6th, 2021

DOI: https://doi.org/10.21203/rs.3.rs-325135/v1

Abstract

The p-arsanilic acid (p-ASA) is widely used in agriculture as a food additive to control parasites. It leaves the body almost unchanged and is subsequently destroyed by environmental factors with the formation of toxic forms of inorganic arsenic. UVA irradiation of p-ASA with the addition of the Fe(III) oxalate complex leads to an effective degradation of the target compound. However, this method needs high concentrations of reagents and the keeping high [oxalate]:[Fe(III)] ratio to maintain proper efficiency of Fe(III) oxalate system. In this work, to overcome these problems, potassium persulfate (PS) was used as an additional oxidizer to improve Fe(III) oxalate system. It was found that the sulfate radical produced upon PS activation reacts readily with both neutral and monoanionic forms of p-ASA yielding corresponding organic cation radical, bimolecular rate constants are $(7.3 \pm 0.6)\times10^9$ and $(2.4 \pm 0.4)\times10^9$ $M^{-1}s^{-1}$, accordingly. Addition of PS allows one to reduce the working concentration of oxalate and achieve the complete degradation of both p-ASA and organic byproducts to the less toxic inorganic As(V) up to 3 ppm of initial p-ASA concentration. Also the proposed approach demonstrates efficiency even for low (< 0.5 ppm) concentrations of p-ASA.

1. Introduction

The widespread use of p-ASA in agriculture has led to the water contamination with inorganic arsenic (As(III) and As(V)), as well as p-ASA itself (Jones 2007, Mangalgiri et al, 2015, Silbergeld and Nachman 2008, Yao et al., 2013). Since p-ASA leaves the body of livestock in almost unchanged form, it is destroyed in the water under the influence of external factors, like pH, temperature and light (Arroyo-Abad et al., 2012, Cortinas et al., 2006, Makris et al., 2008). As inorganic forms of arsenic are toxic to the body, the methods of water purification from p-ASA and similar compounds need to be addressed.

Fe(III) carboxylates are the natural photoactive compounds demonstrating efficient generation of reactive oxygen species (ROS, hydroxyl radicals, mainly) under the action of solar or artificial UV radiation (Faust and Zepp, 1993; Wu and Deng, 2000; Wan et al., 2019; Zuo and Hoigne, 1994). So these complexes are perspective for application in the advanced oxidation processes (AOPs). It has been demonstrated that the combined action of UVA light and Fe (III) - carboxylates could be used for effective degradation of many persistent pollutants, including bisphenols, herbicides, pharmaceuticals, etc. (Chen et al., 2013; Zhong and Yun, 2005; Pozdnyakov et al., 2018; Wan et al., 2018; Wan et al., 2019; Zhou et al., 2004).

Regeneration of active Fe(III) form during the photolysis of Fe(III)-oxalate complexes allows some researches to call such systems as “photocatalytical” though in fact their functioning demands the constant consumption of oxalate ligands as a “sacrificial agent”. This is first, but not the last drawback of Fe(III) oxalate system (Pozdnyakov et al., 2018). The second, photochemical reactions usually require relatively high concentrations of reagents ([Fe(III) > 10^{-4} M, [Ox] > 10^{-3} M, [pollutant] > 10^{-4} M]) (Batista et al., 2014; Nogueira and Guimaraes, 2000; Zhan et al., 2006; Zhou et al., 2004a), which are far beyond of concentrations available under natural conditions. Finally, the Fe(III)-oxalate systems function effectively only with a high ratio of [Ox]: [Fe(III)] (Balmer and Sulzberger, 1999; Graça et al., 2017; Lee et al., 2003;

Zhan et al., 2006; Zhou et al., 2004b) needed for the stabilization and regeneration of the most photoactive Fe(III) form ($[Fe(Ox)_3]^{3-}$) during photolysis.

In our previous work (Tyutereva et al., 2020) the influence of iron oxalate complexes on p-ASA photodegradation was investigated. The photosystem showed a good degradation quantum yield of $^{\cdot}OH$ radical production (f^{308nm} = 0.06) and allows to achieve full degradation of both p-ASA and its aromatic by-products at concentration of pollutant less than 7 μM. It is also demonstrated that during photooxidation significant part (~30%) of inorganic arsenic formed was absorbed by photogenerated Fe(III) complexes.

However, in the application of only the Fe(III) oxalate as photoactive agent the concentrations of oxalate and iron could not be below 0.5 mM and 20 μM, accordingly, to maintain stable degradation rate of p-ASA. To increase the efficiency of this process and to reduce the concentration of reagents, we suggest the use of PS as additional oxidizer.

The activation of PS yields the sulfate radical, a very strong oxidizing agent, which can quickly and more selectively react with aromatic compounds than the hydroxyl radical (Real et al. 2016). PS also reduces the concentration of oxalate and increases its efficiency in photodegradation processes, significantly accelerating the degradation of target compounds. The use of PS allows reducing the amount of "sacrificial" oxalate, while maintaining stabilization and regeneration of the most photoactive form of Fe(III).

Thus, the aim of this work is to study the synergetic effect of the iron oxalate complex and PS on the photodegradation of p-ASA. To shed the light on mechanisms of reactions we directly detected the primary intermediates, determined the rate constants of their reactions with p-ASA and optimized the photolysis conditions to achieve the best degradation of both the target compound and organic byproducts.

2. Materials And Methods

2.1. Chemicals

p-ASA ($C_6H_8AsNO_3$, 98%) was from Aladdin Industrial Corporation (Shanghai, China). The arsenic standards used were arsenious oxide (M&B, Denmark) and sodium arsenate (Fluka, St. Louis, USA). Cetyltrimethylammonium hydroxide (CTAH) solution (Sigma Aldrich), 2,6-pyridinedicarboxylic acid (Sigma Aldrich) and sodium hydroxide (chemically pure) were used for ion chromatography and for pH adjustment, accordingly. Deionized water used to prepare all experimental solutions was obtained with an Ultra Clear water treatment system (SG Wasser, Germany). The pH was measured by the Anion-4100 (Infraspak-Analit, Russia) ionometer.

2.2. Arsenic determination in solutions

Concentration of total arsenic was determined by atomic-emission spectrometry with inductively coupled plasma (ICP-AES). iCap 6000 Duo ICP-AES instrument (Thermo Scientific, USA) with concentric nebulizer and CID detector was applied. The data acquisition and processing was performed by iTEVA (Thermo Scientific, USA) software. The working parameters of ICP-AES were the following: power supply 1150 W, nebulizer flow rate 0.75 L•min^{-1}, cooling gas flow 12 L•min^{-1}. The interference of other elements was eliminated by adding scandium nitrate, $Sc(NO_3)_2$ with concentration of 0.5 ppm, as internal standard, to all tested solutions. ICP-AES in combination with hydride generation technique (HG-ICP-AES) was used to measure As(III) at the concentration level < 0.1 ppm according to the guide (Thermo Scientific, USA).

2.3. Arsenic speciation in solutions

The concentration of inorganic arsenic (As(III) and arsenate As(V) ions), p-ASA and oxalate ions were determined by capillary zone electrophoresis (CZE). Capel 3R CZE system (Lumex Company, Russia) equipped with photometric UV detector was used (Polyakova et al., 2020). Upon the registration of the analysts the following retention order was observed: oxalate, arsenate, p-ASA and arsenite. The correctness of peaks assignment was confirmed by using corresponding individual standards. Determination of the total arsenic content to assess the balance of the element was performed by ICP-AES.

2.4. Optical spectroscopy and photolysis setups

Agilent 8453 spectrophotometer (Agilent Technologies, USA) was used to record optical spectra. The stationary photolysis experiments were carried out in quartz cells with a total volume of 10 ml and an optical path length of 5 cm at normal oxygen content in solution. Excimer XeCl lamp (308 nm) manufactured by the Institute of High Current Electronics, SB RAS, Tomsk, Russia (Sosnin et al., 2006) was used as a source of a stationary radiation.

Time-resolved experiments were performed using a conventional laser flash photolysis setup (Pozdnyakov et al., 2006). Quartz cells with a total volume of 3 ml and an optical path length of 1 cm at normal oxygen content in solutions were applied. A tunable LS-2137U laser (Lotis, Belarus) with an excitation wavelength of 355 or 266 nm was used as excitation source with pulse duration of about 6 ns, and pulse energy from 1 to 15 mJ. The optical sensitivity of the setup is up to 5×10^{-4}, the spectral range is 270–800 nm, and the temporal resolution is 50 ns. For the numerical calculations of kinetic curves, the differential equations were solved by means of thef fourth-order Runge-Kutta method using RUNGE (developer Yu.V. Ivanov) software (Pozdnyakov et al., 2008).

2.5. Photodegradation studies

The photodegradation of p-ASA was also studied by LC 1200 high performance liquid chromatography (HPLC) system (Agilent Technologies, USA) equipped with a diode array detector from the Center of Collective Use «Mass spectrometric investigations» SB RAS. Separations were performed using an Agilent Zorbax Eclipse RapidResolution XBD-C18 column (4.6 × 100 mm, 80 Å, 1.8 μm) in isocratic elution

of mobile phase (5% of acetonitrile and 0.1% v/v of formic acid) with the flow rate 0.5 mL/min. The injection volume was 80 µL. Retention time of p-ASA was 2.75 min. Concentration of total aromatics (TAR) was estimated by integration of all peaks in a chromatogram at 250 nm corresponding to the initial compound and its photoproducts. Analysis of the obtained results was performed using Agilent ChemStation software.

3. Results And Discussion

3.1 Laser flash photolysis of potassium persulfate in the presence of p-ASA

To generate a sulfate radical and study its reaction with p-ASA monoanion (pKa values: 2.00, 4.02, and 8.92 (Jaafar, 2001)), the flash (266 nm) photolysis of potassium persulfate at pH 7 was performed. To minimize a contribution of the intrinsic pASA photochemistry (Tyutereva et al., 2019) we used laser pulses of low energy (typically, around 1 mJ/pulse). Figure 1 demonstrates the evolution of the absorption spectra of PS in aqueous solution in the presence of p-ASA at pH 7 and the kinetic curves for three characteristic wavelengths. Immediately after the laser pulse, a wide absorption band was observed with a maximum at 440 nm, corresponding to the spectrum of the $SO_4^{\bullet-}$ radical (Ivanov et al., 2000). Then this band narrows and grows in amplitude within first two microseconds with a subsequent decrease of the signal on the time scale of tens of microseconds (Fig. 1).

The secondary intermediate observed at time delays more than 3 µs after the laser pulse was assigned to the p-ASA radical-cation ($RNH_2^{+\bullet}$) formed in the reaction of a sulfate radical with a p-ASA (2). A similar intermediate, with an absorption maximum at 430 nm, was registered earlier in the direct photolysis of p-ASA (Tyutereva et al., 2019).

$$SO_4^{-\bullet} + SO_4^{-\bullet} \xrightarrow{k_1} S_2O_8^{2-} \quad (1)$$

$$SO_4^{-\bullet} + RNH_2 \xrightarrow{k_2} RNH_2^{+\bullet} + SO_4^{2-} \quad (2)$$

The decay of $RNH_2^{+\bullet}$ radical at the initial times can be described by a first-order equation (3) with an effective rate constant k_3:

$$RNH_2^{+\bullet} \xrightarrow{k_3} P \quad (3)$$

Since the $SO_4^{-\bullet}$ radical (Ivanov et al., 2000) undergoes effective recombination in reaction (1), an analytical solution for the schemes (1-3) cannot be realized. However, kinetic curves of transient absorption decay were calculated numerically by the 4th order Runge-Kutta method using the kinetic schemes (1-3) (see Fig. S1 and additional information in ESI for details). The influence of p-ASA concentration on the sulfate radical decay is the most pronounced at 490 nm (Fig. 2). For calculations we used the absorption coefficient of the sulfate radical at 490 nm, $\varepsilon(SO_4^{2-\bullet}) = 1000\ M^{-1}cm^{-1}$ (Ivanov et al.,

2000) and the recombination constant of this radical, $2k_2 = 2.9\times10^9$ $M^{-1}s^{-1}$, determined from the second-order fit of the kinetic curve at 490 nm in the absence of p-ASA (Fig. 2, curve 1); these parameters were fixed during the subsequent calculations. The remaining parameters were fitted to achieve the best agreement between the calculated and experimental curves in a wide range of p-ASA concentrations (Fig. 2).

The numerical calculations gave the value of the rate constant for the reaction of $SO_4^{-\bullet}$ radical with p-ASA monoanion as $k_2 = (2.4 \pm 0.4)\times10^9$ $M^{-1}s^{-1}$; the observed decay rate constant of $RNH_2^{+\bullet}$ radical and its absorption coefficient at 490 nm as $k_3 = (5.7 \pm 1.5)\times10^3$ $M^{-1}s^{-1}$ and $e(RNH_2^{+\bullet}) = (3.4 \pm 0.5)\times10^2$ $M^{-1}cm^{-1}$, respectively. At pH 3 the reaction rate constant of the sulfate radical with the neutral form of p-ASA is $k_2 = (7.3 \pm 0.6) \times10^9$ $M^{-1}s^{-1}$ that is three times greater than that obtained for the anionic one (Fig. S2). This indicates the strong influence of Coulomb repulsion during the interaction of two negatively charged species at pH 7. However both rate constants are close to diffusion-controlled limit, so one can conclude that $SO_4^{-\bullet}$ radical could readily oxidize p-ASA at a wide pH range even at low concentration of the target molecule.

3.2 Stationary photolysis of the $Fe(Ox)_3^{3-}$ complex with PS in the presence of p-ASA.

In our previous article (Tyutereva et all., 2020) we demonstrated that at neutral pH the Fe(III) oxalate complexes effectively generate $^{\bullet}OH$ radical under UV irradiation, which reacts with p-ASA with high rate constant, $(8.6 \pm 0.5) \times 10^9$ $M^{-1}s^{-1}$. Subsequent oxidation of organic radical formed leads to complete degradation of both p-ASA and basic aromatic photoproducts with formation of inorganic As(V) mainly, under optimal conditions. It is also worth to note, that p-ASA has own photochemistry under 308 nm irradiation but it is negligible in our experimental conditions due to high absorption and photoactivity of Fe(III) complexes.

The presence of both Fe(III) oxalate and PS in the solution accelerates the photodegradation of p-ASA and gives an opportunity to reduce the working concentration of oxalate ions in the solution (from 0.5 to 0.12 mM) without changes in the high degradation efficiency of not only the target compound but the aromatic photoproducts as well (Fig. 3). This can be explained by the catalytic decomposition of PS by photogenerated Fe(II) ions with the regeneration of the initial Fe(III) oxalate complex and the formation of additional oxidative sulfate radical:

$$Fe(II) + S_2O_8^{2-} = Fe(III) + SO_4^{2-} + SO_4^{-\bullet} \quad (4)$$

Addition of PS also allows to oxidize p-ASA at high concentration of the pollutant that cannot be done in the presence of iron oxalate alone. Figure 4 shows the dependence of the yield of different arsenic species on the irradiation time of p-ASA – Fe(III) oxalate system in the presence and absence of PS at initial concentration of p-ASA about 3 ppm (4×10^{-5} M). Without PS only a partial (about 50%) degradation of p-ASA was observed after 40 min of irradiation (Fig. 4A). The total content of arsenic including p-ASA

and inorganic species at the end of irradiation (~1.7 ppm) was significantly less than the total arcenic concentration (~2.8 ppm) before irradiation that indicates an accumulation of some organic arcenic byproducts with questionable toxicity.

In the presence of PS (Fig. 4B) the complete degradation of p-ASA was observed with generation of As(V) mainly, which can be removed by standard water treatment procedures (Vircikova et all., 1996; Lawrence and Higgs, 1999). It worth to note that the concentration of As(V) measured by CZE method shows evident decrease after 20 minutes of irradiation comparatively with the experiment withot PS (Fig. 4B). To explain such puzzling effect the test experiments with model As(V) - Fe(III) oxalate – PS system without and with irradiation were carried out under the same conditions.

Figure 5A demonstrates the difference between actual (by preparation) concentration of As(V) measured using methods of ICP-AES and CZE before and after irradiation. Prior to irradiation both methods give results consistent with each other and actual As(V) concentration (Fig. 5A). In the case of photolysed samples, ICP-AES shows no influence of irradiation on the measured concentrations of As(V), while CZE demonstrates a pronounced decrease of As(V) by 0.7 – 2 ppm, depending on the initial arsenic content. This discrepancy increases with exposure (Fig. 5B) that gives a right to assume that a portion of As(V) transforms into another form or product, which is out of registration by CZE, e.g., conjugate or complex, on account of Fe(III)-oxalate degradation. Analogous loss of As(V) measured by CZE was reported in our previous work (Tyutereva et al., 2020) where oxidation of p-ASA was studied in Fe(III)-oxalate system in the absence of PS. According to (Wang et all., 2020), this unknown product is most likely an As(V) – ferric oxyhydroxides colloid.

Another argument for the assumption that part of arsenic is sorbed on photogenerated iron oxyhydroxides are the results of total As determination using ICP-AES analysis of undisturbed samples few days after photolysis (Fig. S3). The total arsenic concentration is restored by a shaking of samples prior the measurements. Figure 5B also illustrates this effect (curves 1 and 1'). This important observation indicates that both processes including p-ASA oxidation and As(V) sorption occurs during a single photochemical process. The significance of this effect for further application of this photochemical approach for p-ASA removal from natural waters is in the reduction of the number and the cost of water purification steps. We intend to continue research in this prospective direction in the nearest future.

Assuming that p-ASA is completely converted to inorganic forms of arsenic we can estimate the loss of As(V) in CZE measurements after 20 and 40 min of irradiation, accordingly. Result was lower that one predicted by photolysis of the model system with As(V) (³1 ppm, Fig. 5B). However, it should be taken into account that in the model system ROS, generated by excitation of Fe(III) oxalate, react immediately with the complex itself. In the presence of p-ASA these active species firstly react with target pollutant and start the degradation of complex only at the final stage of photolysis. So, we can expect the stabilization of Fe(III)-oxalate system in presence of p-ASA as compared with As(V).

After correction of As(V) concentrations measured by CZE, we can conclude that in the presence of 1 mM PS the complete degradation of p-ASA to inorganic arsenic occurs at concentrations of p-ASA up to 3 ppm. The ratio of As(III)/As(V) formed during p-ASA oxidation depends on the initial concentration of the pollutant. Figure 6 demonstrates the arsenic species distribution in solution after 20 min of irradiation depending on the starting concentration of p-ASA. Almost complete conversion of p-ASA to inorganic arsenic could be seen (Fig. 6). Another important result is the decrease of As(III)/As(V) ratio from 0.21 to negligible value (Fig. 6, inset) with the lowering of p-ASA concentration from 3.3 to 0.44 ppm. Apparently, at low p-ASA concentrations all photogenerated As(III) is completely oxidized by PS. High concentrations of p-ASA lead to higher consumption of PS that, in turn, results in incomplete degradation of photogenerated As(III). At real concentration of the organic arsenicals in contaminated surface water (~ tens ppb, Mangalgiri et all., 2015) all p-ASA is expected to fully converts to As(V) in Fe(III)-oxalate – PS system, which significantly reduces the toxic effect of p-ASA on the environment.

Conclusions

Joint oxidation of p-ASA by $^{\bullet}OH$ and $SO_4^{-\bullet}$ radical was studied by the combination of steady-state and time-resolved optical methods. The rate constant for the reaction of $SO_4^{-\bullet}$ radical with p-ASA monoanion was calculated as $k_1 = (2.4 \pm 0.4)\times10^9$ $M^{-1}s^{-1}$. At pH 3 the neutral form of p-ASA reacts with $SO_4^{-\bullet}$ radical three times faster ($k_2 = (7.3 \pm 0.6) \times10^9$ $M^{-1}s^{-1}$). This indicates the strong influence of Coulomb repulsion on the interaction of two negatively charged partners at neutral pH. It was shown that addition of PS to Fe(III)-oxalate system has several advantages for p-ASA photooxidation. First, the presence of PS significantly reduces the concentration of oxalate required for complete p-ASA degradation. Second, higher degradation efficiency of the target compound leads to lower exposure doses and total time for photolysis. Third, the predominant formation of As(V) reduces the number and cost of subsequent purification cycles. The proposed approach demonstrates efficiency even for low concentrations of p-ASA. Also the observed effect of partial sorption of As(V) on photogenerated Fe(III) species formed upon p-ASA photooxidation opens a new opportunities of Fe(III)-oxalate – PS system application in water purification processes though further studies of the adsorption prosesses are necessary for their effective use in the real applications.

Declarations

Ethics approval and consent to participate – "Not applicable"

Consent for publication - "Not applicable"

Availability of data and materials - "Not applicable"

Competing interests - "The authors declare that they have no competing interests"

Funding:Russian Science Foundation (Grant RSF-NSFC № 21-43-00004) and the National Natural Science Foundation of China (Grant NSFC-RSF 22061132001)

Authors' contributions:Y.E. Tyutereva: Investigation, P.S. Sherin: Writing - Original Draft, E.V. Polyakova: Investigation, V.P. Grivin: Methodology, Software, V.F. Plyusnin: Funding acquisition, O.V. Shuvaeva: Investigation, Methodology, J. Xu: Conceptualization, Funding acquisition, F. Wu: Conceptualization, I.P. Pozdnyakov: Conceptualization, Investigation, Writing - Original Draft, Writing - Review & Editing

Acknowledgements

The financial support of the Russian Science Foundation (Grant RSF-NSFC № 21-43-00004) and the National Natural Science Foundation of China (Grant NSFC-RSF 22061132001) is gratefully acknowledged.

References

1. Arroyo-Abad U, Mattusch J, Moder M, Elizalde-Gonzalez MP, Matysik FM Identification of degradation products of phenylarsonic acid and o-arsanilic acid in contact with suspensions of soils of volcanic origin// Talanta, 99 (2012). 310–315. DOI: 10.1016/j.talanta.2012.05.057
2. Balmer ME, Sulzberger B (1999) Atrazine degradation in irradiated iron oxalate systems: effects of pH and oxalate//. Environ Sci Technol 33:2418–2424. DOI:https://doi.org/10.1021/es9808705
3. Batista APS, Cottrell BA, Pupo Nogueira RF (2014) Photochemical transformation of antibiotics by excitation of Fe(III)-complexes in aqueous medium. J Photochem Photobiol A: Chem 274:50–56. DOI:10.1016/j.jphotochem.2013.09.017
4. Benkelberg H-J, Warneck P (1995) Photodecomposition of iron(III) hydroxo and sulfato complexes in aqueous solution: wavelength dependence of OH and SO4- quantum yields. J Phys Chem 99:5214. DOI:10.1021/j100014a049
5. Buxton GV, Greenstock CL, Helman WP, Ross AB - Critical Review of Rate Constants for Reactions of Hydrated Electrons, Hydrogen Atoms and Hydroxyl Radicals (•OH/•O–) in Aqueous Solution// Phys. Chem. 17 (1988) – 513–531. DOI: 10.1063/1.555805
6. Chen Y, Zhang K, Zuo Y, Direct and indirect photodegradation of estriol in the presence of humic acid, nitrate and iron complexes in water solutions. Sci Total Environ 463–464 (2013) 802–809, doi:10.1016/j.scitotenv.2013.06.026
7. Cortinas I, Field JA, Kopplin M, Garbarino JR, Gandolfi AJ, Sierra-Alvarez R (2006) Anaerobic biotransformation of roxarsone and related N-substituted phenylarsonic acids//. Environ Sci Technol 40:2951–2957. DOI:10.1021/es051981o
8. Faust BC, Zepp RG (1993) Photochemistry of aqueous iron (III)-polycarboxylate complexes: Roles in the chemistry of atmospheric and surface waters. Environ SciTechnol 27:2517–2522. DOI:10.1021/es00048a032

9. Graça CAL, Correia de Velosa A, Teixeira ACSC (2017) Role of Fe(III)-carboxylates in AMZ photodegradation: a response surface study based on a Doehlert experimental design//. Chemosphere 184:981–991. DOI:10.1016/j.chemosphere.2017.06.013
10. Ivanov KL, Glebov EM, Plyusnin VF, Ivanov YuV, Grivin VP, Bazhin NM (2000) Laser flash photolysis of sodium persulfate in aqueous solution with additions of dimethylformamide. J Photochem Photobiol A: Chem 133:99–104. DOI:10.1016/S1010-6030(00)00218-5
11. Jeong J, Yoon J (2005) pH effect on OH radical production in photo/ferrioxalate system. Water Res 39:2893–2900. DOI:10.1016/j.watres.2005.05.014
12. Jones FT. A broad view of arsenic// Poult Sci, 86 (2007). 2–14. DOI:10.1093/ps/86.1.2
13. Lawrence RW, Higgs SATW (1999) Removing and stabilizing As in acid mine water. JOM 51:27–29. DOI:https://doi.org/10.1007/s11837-999-0154-z
14. Lee Y, Jeong J, Lee C, Yoon J (2003) Influence of various reaction parameters on 2,4-D removal in photo/ferrioxalate/H2O2 process. Chemosphere 51:901–912. DOI:https://doi.org/10.1016/S0045-6535(03)00044-4
15. Li J, Mailhot G, Wu F, Deng NS (2010) Photochemical efficiency of Fe(III)-EDDS complex: OH radical production and 17 beta-estradiol degradation. J Photochem Photobiol A: Chem 212:1–7. DOI:10.1016/j.jphotochem.2010.03.001
16. Li S, Xu J, Chen W, Yu Y, Liu Z, Li J, Wu F (2016) Multiple transformation pathways of p-arsanilic acid to inorganic arsenic species in water during UV disinfection. Environ Sci 47:39–48. DOI:10.1016/j.jes.2016.01.017
17. Mangalgiri KP, Adak A, Blaney L (2015) Organoarsenicals in poultry litter: Detection, fate, and toxicity. Environ Int 75:68–80. DOI:10.1016/j.envint.2014.10.022
18. Makris KC, Quazi S, Punamiya P, Sarkar D, Datta R (2008) - Fate of arsenic in swine waste from concentrated animal feeding operations//. Environ Qual 37:1626–1633. DOI:10.2134/jeq2007.0479
19. Nogueira RP, Guimaraes JR (2000) Photodegradation of dichloroacetic acid and 2,4-dichlorophenol by ferrioxalate/H_2O_2 system. Water Res 34:895–901. DOI:https://doi.org/10.1016/S0043-1354(99)00193-1
20. Polyakova EV, Shuvaeva OV, Koscheeva OS, Tyutereva YE, Pozdnyakov IP, Capillary zone electrophoresis as a simple approach for the study of p-arsanilic acid transformation in the process of photolytic degradation, Electrophoresis, 2020, https://doi.org/10.1002/elps.202000262
21. Pozdnyakov IP, Glebov EM, Plyusnin VF, Grivin VP, Ivanov YuV, Bazhin NM, Vorobjev DYu (2000) Mechanism of $Fe(OH)^{2+}$(aq) Photolysis in Aqueous Solution. Pure Appl Chem 72:2187–2197. DOI:10.1351/pac200072112187
22. Pozdnyakov IP, Plyusnin VF, Grivin VP, Vorobyev DY, Bazhin NM, Vauthey E (2006) - Photolysis of sulfosalicylic acid in aqueous solutions over a wide pH range//. J Photochem Photobiol A: Chem 181:37–43. DOI:10.1016/j.jphotochem.2005.10.030

23. Pozdnyakov IP, Kel OV, Plyusnin VF, Grivin VP, Bazhin NM (2008) New Insight into Photochemistry of Ferrioxalate. J Phys Chem A 112:8316–8322. DOI:10.1021/jp8040583
24. Pozdnyakov IP, Sherin PS, Bazhin N, Plyusnin V (2018) $[Fe(Ox)_3]^{3-}$ complex as a photodegradation agent at neutral pH: advances and limitations. Chemosphere 195:839–846. DOI:10.1016/j.chemosphere.2017.12.096
25. Silbergeld EK, Nachman K (2008) The environmental and public health risks associated with arsenical use in animal feeds//. Ann N Y Acad Sci 1140:346–357. DOI:10.1196/annals.1454.049
26. Sosnin E, Oppenlander T, Tarasenko V Applications of capacitive and barrier discharge excilamps in photoscience// Photochem. Photobiol. C: Photochem. Rev., 7 (2006) – 145–163. DOI: 10.1016/j.jphotochemrev.2006.12.002
27. Tyutereva YuE, Sherin PS, Parkhats MV, Liu Z, Xu J, Wu F, Plyusnin VF, Pozdnyakov IP New insights into mechanism of direct UV photolysis of p-arsanilic acid, Chemosphere, 220 (2019) 574–581, DOI: 10.1016/j.chemosphere.2018.12.179 (Tyutereva et al., 2019a)
28. Sherin TYuE, Liu PS, Plyusnin Z, Pozdnyakov VF I.P., UVC-induced photodegradation of p-arsanilic acid assisted by humic substances, Mendeleev Commun., 29 (2019) 512–514. DOI: 10.1016/j.mencom.2019.09.011 (Tyutereva et al., 2019b)
29. Sherin TYuE, Polyakova PS, Koscheeva EV, Plyusnin OS,GVP, Shuvaeva VF, Pozdnyakov OV I. P., Photodegradation of para-arsanilic acid mediated by photolysis of iron(III) oxalate complexes, Chemosphere, 261 (2020) 127770, DOI: https://doi.org/10.1016/j.chemosphere.2020.127770
30. Vircikova E, Palfy P, Molnar L, Lech P (1996) As(III) elimination from solutions and As-precipitates charac-teristic. Miner Slov 28(5):406–408
31. Vaclavikova M, Gallios GP, Hredzak S et al (2008) Removal of arsenic from water streams: an overview of available techniques. Clean Techn Environ Policy 10:89–95. https://doi.org/10.1007/s10098-007-0098-3
32. Wang L, Zhang C, Wu F, Deng N, Glebov EM, Bazhin NM (2006) Determination of hydroxyl radicals from photolysis of Fe(III)-pyruvate complexes in homogeneous aqueous solution. Reaction Kinetics Catalysis Letters 89:183–192. DOI:10.1007/s11144-006-0101-8
33. Wang P, He X, Zhang W, Ma J, Jiang J, Huang Z, Cheng H, Pang S, Zhou Y, Zhai X (2020) Highly efficient removal of p-arsanilic acid with Fe(II)/peroxydisulfate under near-neutral conditions. Water Res 177:115752. DOI:10.1016/j.watres.2020.115752
34. Wu F, Deng N. Photochemistry of hydrolytic iron (III) species and photoinduced degradation of organic compounds. A minireview, Chemosphere, 41 (2000) 1137. DOI: 10.1016/S0045-6535(00)00024-2
35. Xie X, Hu Y, Cheng H (2016) Mechanism, kinetics, and pathways of self-sensitized sunlight photodegradation of phenylarsonic compounds//. Wat Res 96:136–147. DOI:10.1016/j.watres.2016.03.053
36. Xu J, Shen X, Wang D, Zhao C, Liu Z, Pozdnyakov IP, Wu F, Xi J (2018) Kinetics and mechanisms of pH-dependent direct photolysis of p-arsanilic acid under UV-C light//. Chem Eng 336:334–341.

DOI:10.1016/j.cej.2017.12.037

37. Yao L, Huang L, He Z, Zhou C, Li G. Agric (2013) Occurrence of arsenic impurities in organoarsenics and animal feeds//. Food Chem 61:320–324. DOI:10.1021/jf3045022
38. Zhan MJ, Yang X, Xian QM, Kong LR (2006) Photodegradation of bisphenol A in Fe(III)-oxalate complexes soluion. J Environ Sci China 18:771–776
39. Zhang C, Wang L, Wu F, Deng N (2006) Quantitation of Hydroxyl Radicals from Photolysis of Fe(III)-Citrate Complexes in Aerobic. Environ Sci Pollut Res 13:156–160. DOI:10.1065/espr2005.10.287
40. Zhu X-D, Wang Y-J, Liu C, Qin W-X, Zhou D-M Kinetics, intermediates and acute toxicity of arsanilic acid photolysis// Chemosphere, 107 (2014). 274–281. DOI: 10.1016/j.chemosphere.2013.12.060
41. Zhou D, Wu F, Deng N, Xiang W, Photooxidation of bisphenol A (BPA) in water in the presence of ferric and carboxylate salts, Water Res. 38 (2004a) 4107–4116, DOI:10.1016/j.watres.2004.07.021
42. Zhou D, Wu F, Deng N (2004b) Fe(III)-oxalate complexes induced photooxidation of diethylstilbestrol in water. Chemosphere 57:283–291. DOI:https://doi.org/10.1016/j.chemosphere.2004.05.043
43. Zuo Y, Hoigne J (1994) Photochemical decomposition of oxalic, glyoxalic and pyruvic acid catalyzed by iron in atmospheric waters. Atmos Environ 28:1231–1239. DOI:10.1016/1352-2310(94)90270-4

Figures

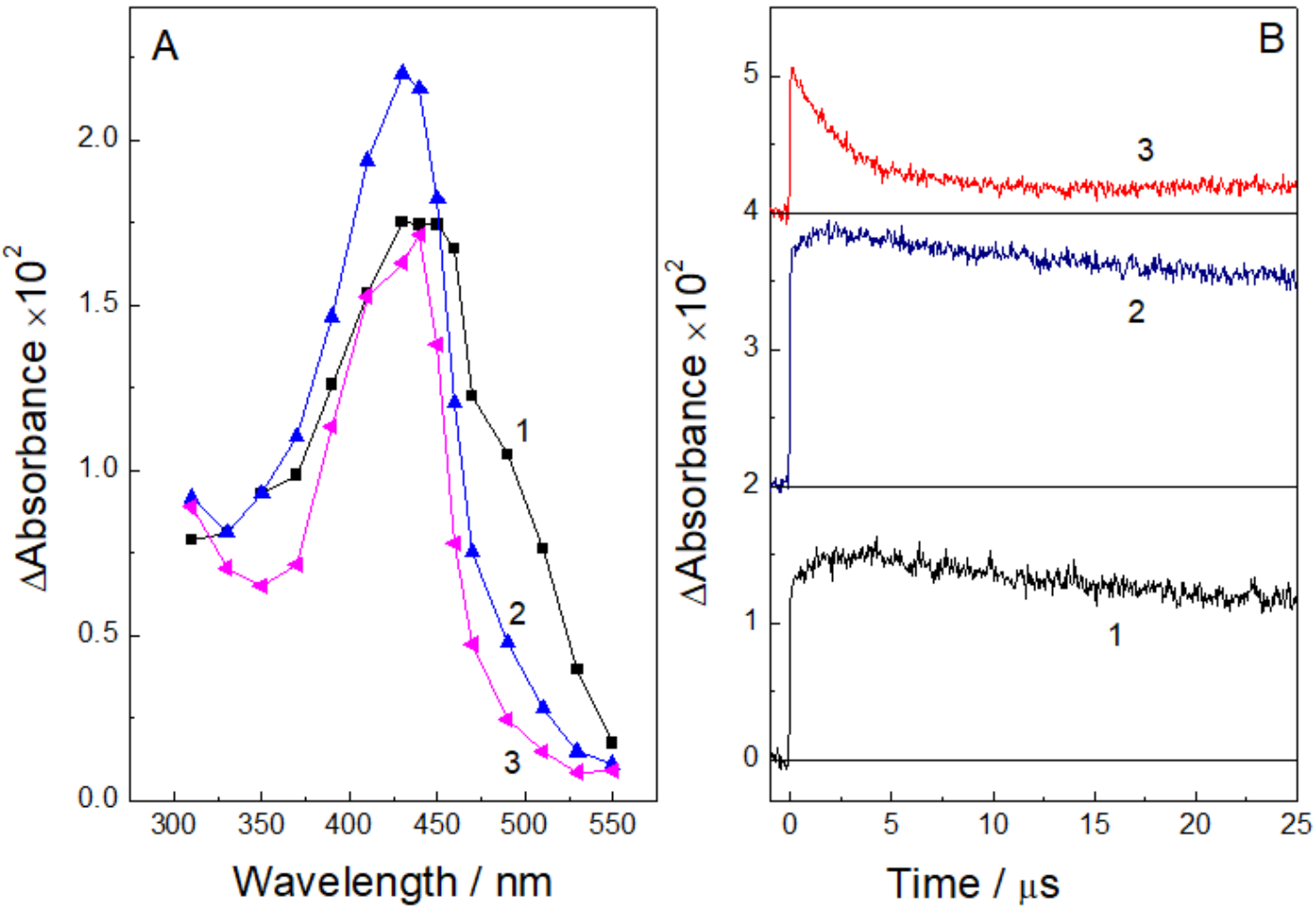

Figure 1

Laser Flash Photolysis (266 nm) of PS (0.045 M) in the presence of 10-4 M p-ASA. (A) – absorption spectra of intermediate through 0.05 (1), 3 (2) and 48 (3) μs after excitation; (B) - kinetic curves at three characteristic wavelengths of 390 (1), 450 (2) and 490 nm (3). Excitation energy 1.3 mJ /pulse, pH = 7.

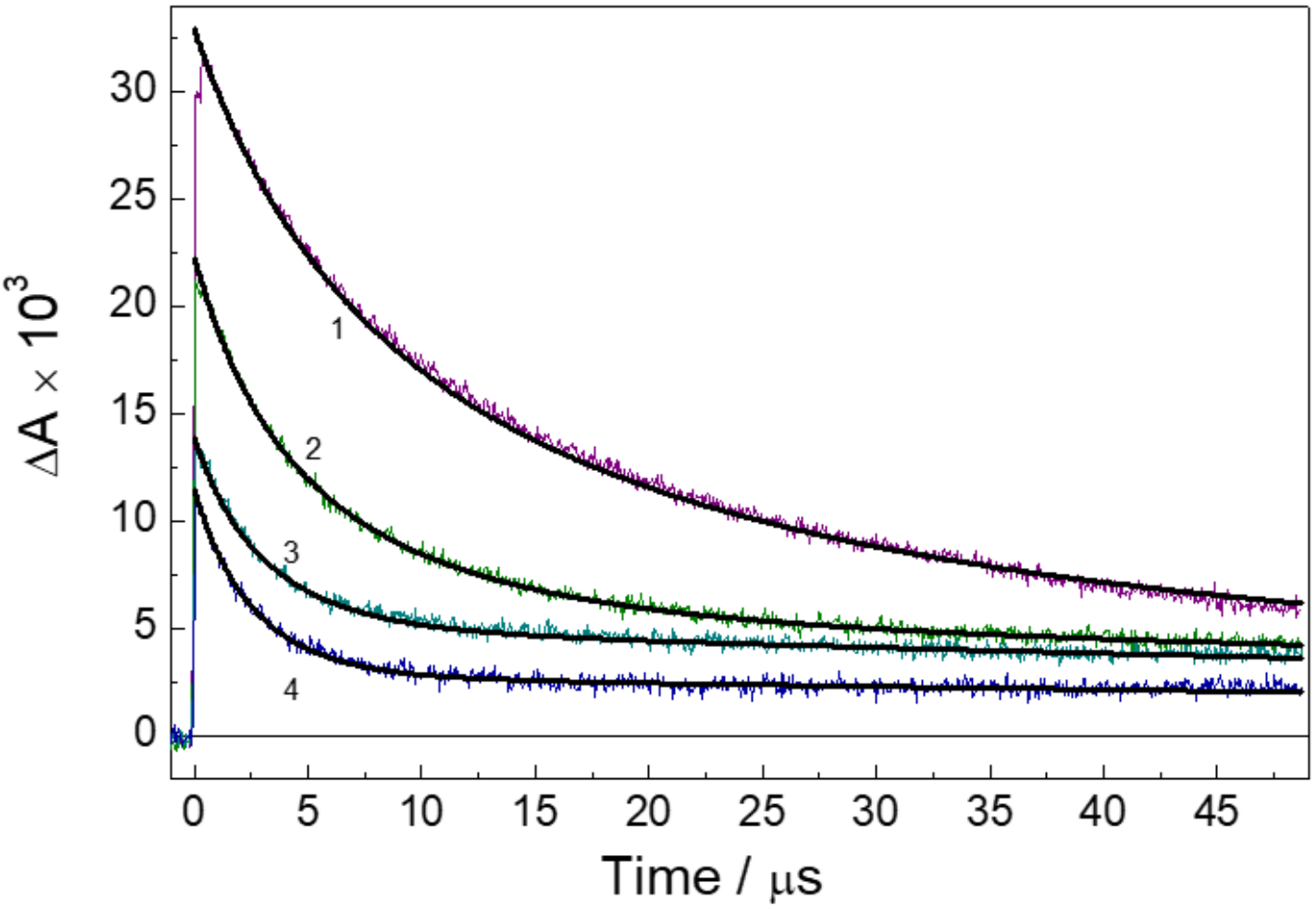

Figure 2

Laser Flash Photolysis (266 nm) of 0.045 M PS in the presence of p-ASA at pH = 7. Kinetic curves (490 nm) at the concentrations of p-ASA: 0 M (1), 5.7× 10-5 M (2), 1.2×10-4 M (3) and 2.1×10-4 M (4), respectively. Smooth curves are the results of numerical modeling by the 4th order Runge-Kutta method according to the kinetic schemes (1-3).

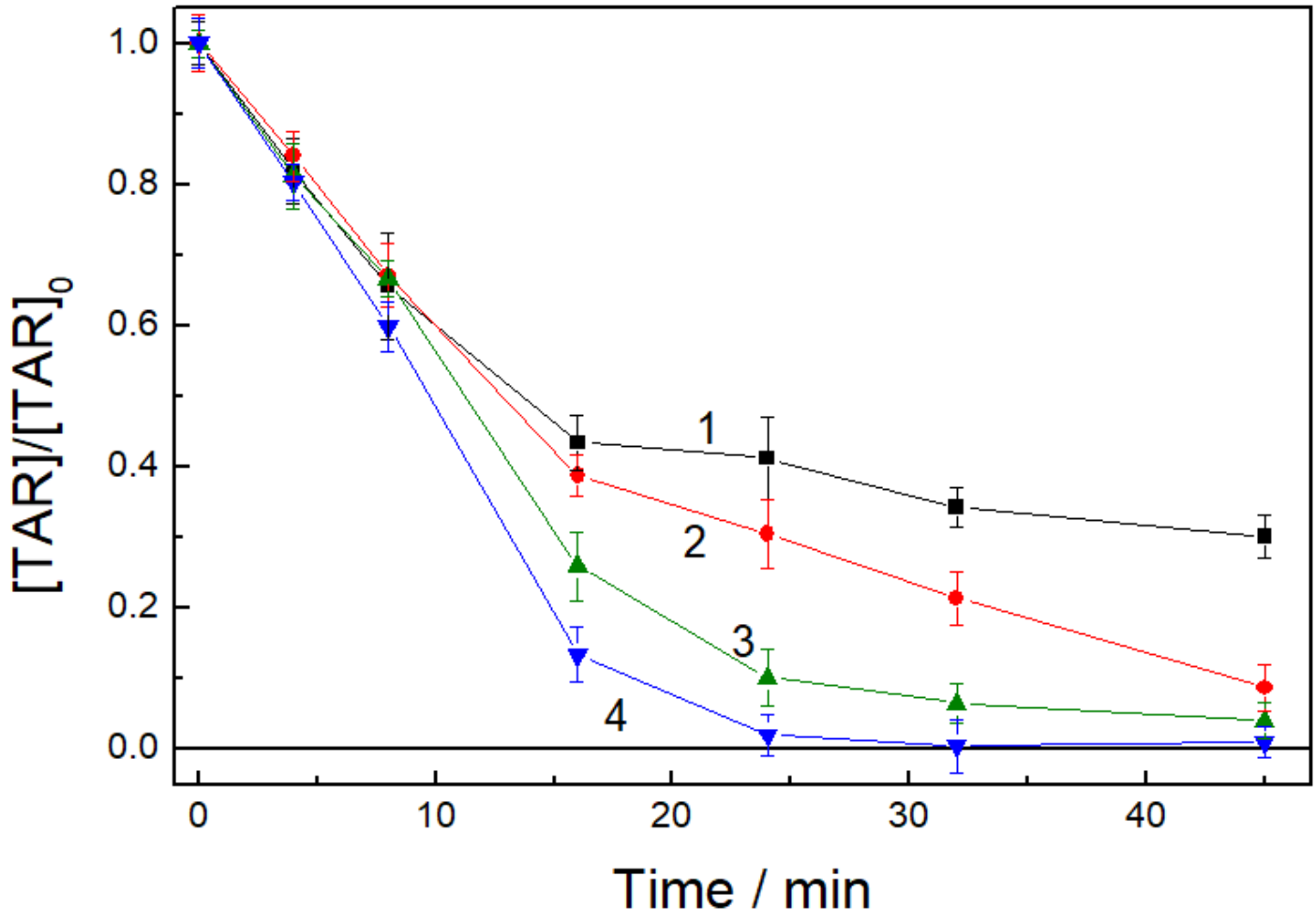

Figure 3

The effect of the initial concentration of PS: 0 M (1), 1×10-4 M (2), 3.5×10-4 M (3) and 10×10-4 M (4) on evolution of total aromatics (TAR) during photolysis. [p-ASA] = 7×10-6 M (0.53 ppm), [Fe(III)] = 2×10-5 M, [oxalate-ion] = 1.2×10-4 M, pH = 6.7.

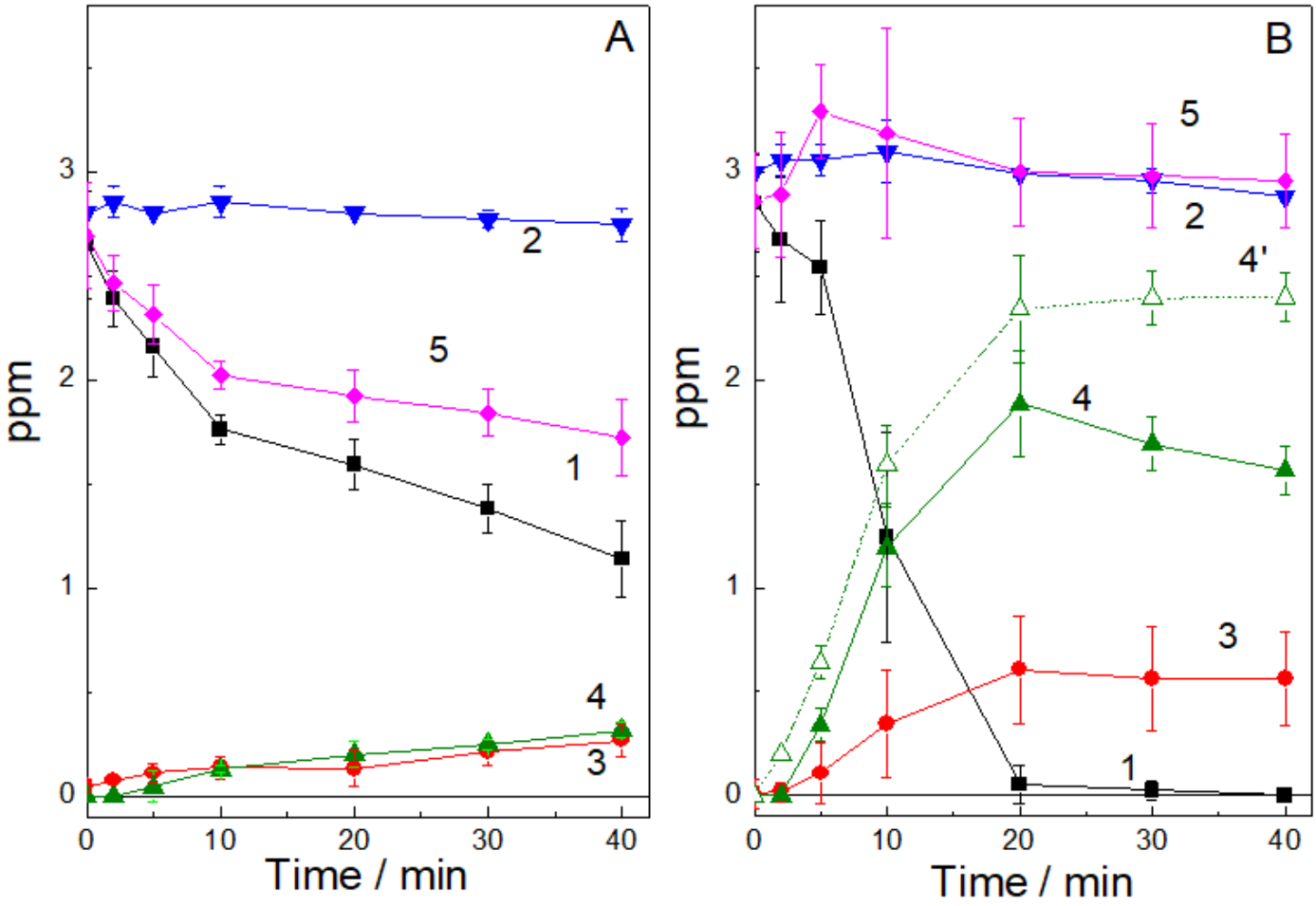

Figure 4

Temporal dynamics of arsenic species during UV photolysis of p-ASA in presence of Fe(III) oxalate without (A) and with (B) PS: p-ASA (1), total arsenic (2), As (III) (3), As (V) (4), As(V) corrected to CZE signal decrease (4'), sum of p-ASA, As(III) and As(V) corrected to CZE signal decrease (5). [Fe(III)] = 2×10-5 M, [Oxalate] = 1.2×10-4 M, [PS] = 0 and 10-3 M, accordingly.

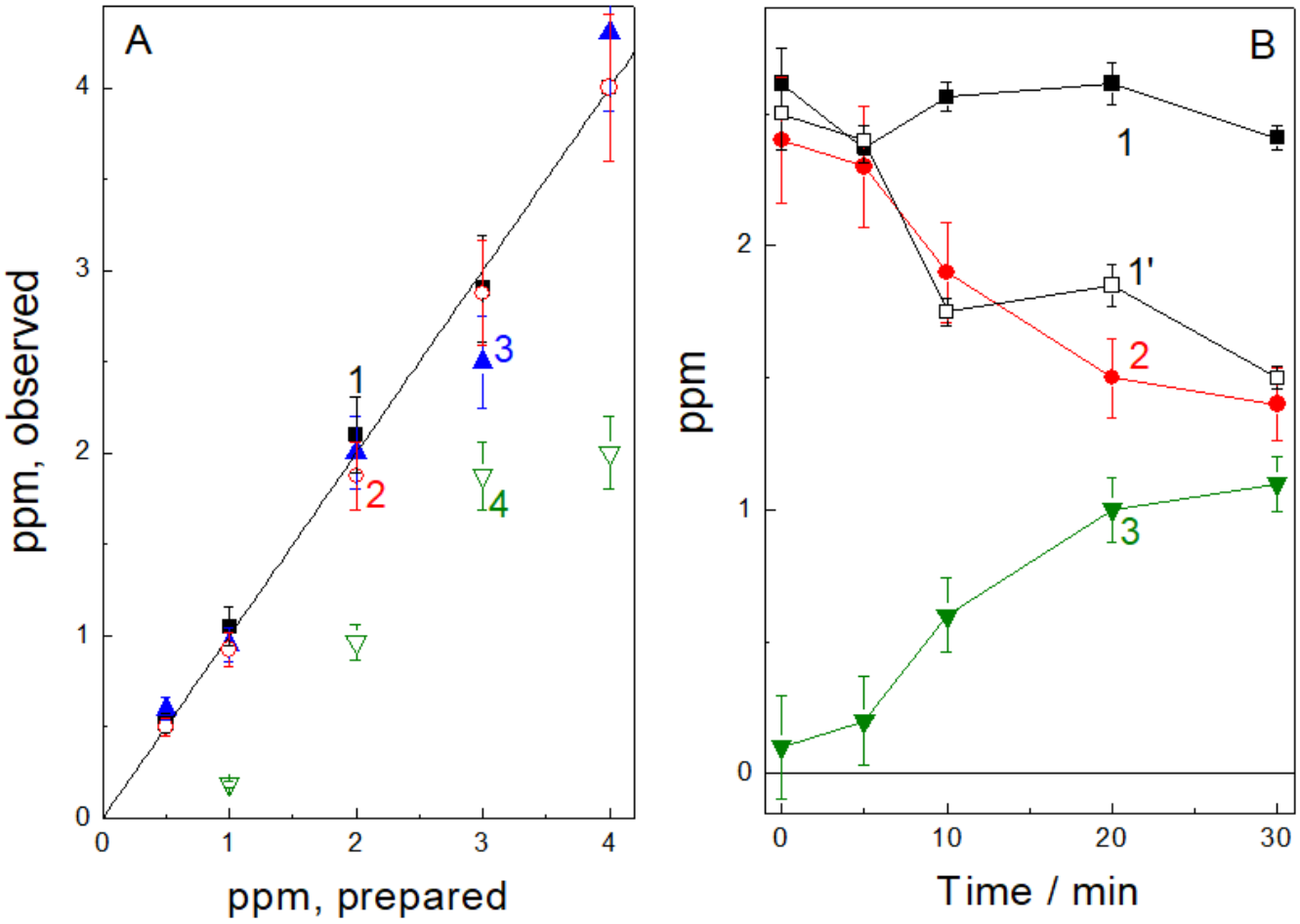

Figure 5

(A) - comparison of As(V) concentration measured by ICP-AES (1,3) and CZE methods (2,4) without (1,2) and after 20 min irradiation (3,4). (B) – change of As(V) concentration measured by ICP-AES with (1) and without shaking (1') of the samples, by CZE methods (2) and the difference (3) during irradiation at 308 nm of 2.5 ppm of As(V) in the presence of Fe(III)-oxalate and PS. [Fe(III)] = 2×10-5 M, [Oxalate] = 1.2×10-4 M, [PS] = 10-3 M, accordingly.

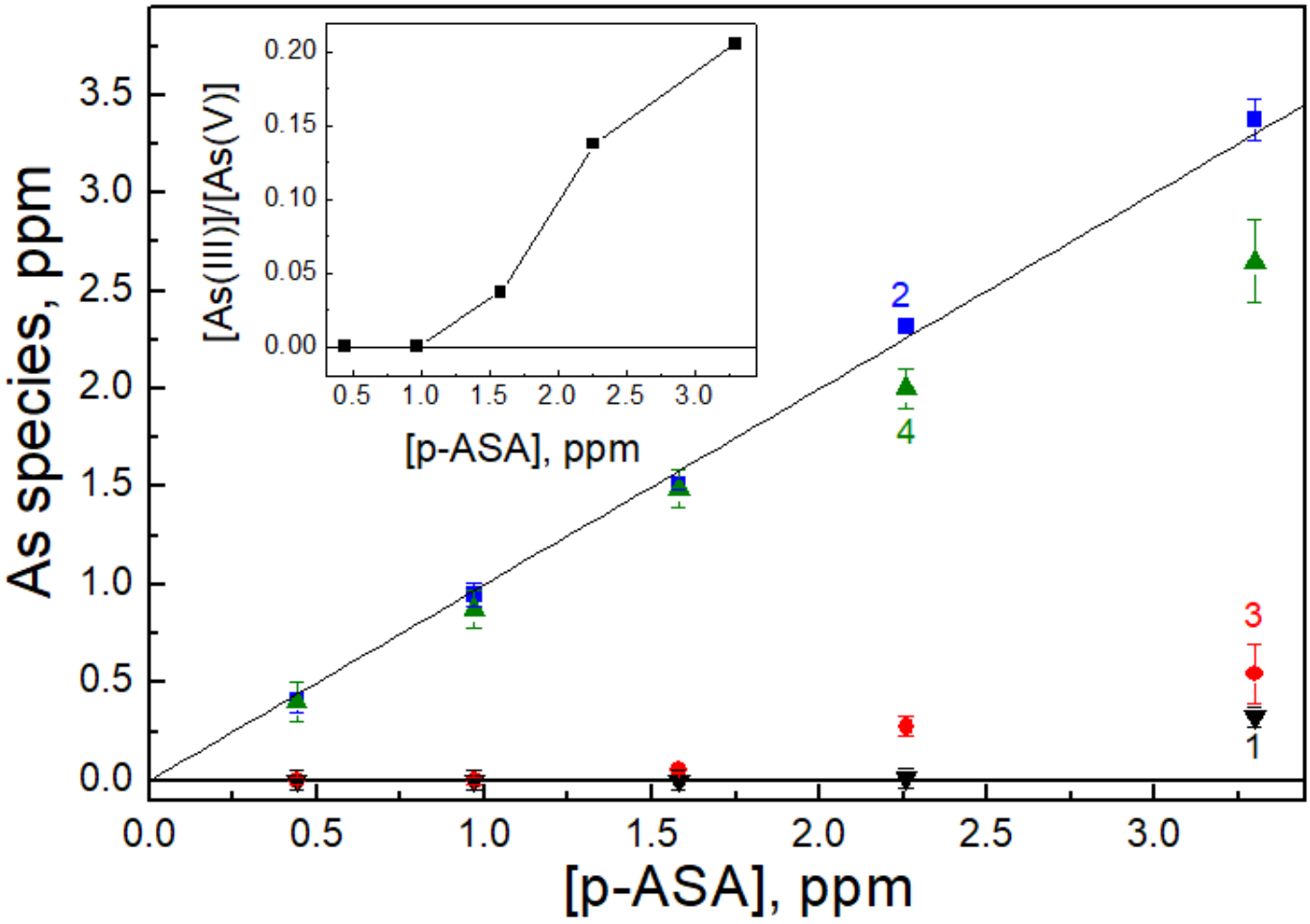

Figure 6

Yield of arsenic species after 20 min of UV photolysis of p-ASA in presence of Fe(III) oxalate and PS: p-ASA (1), total arsenic (2), As (III) (3), As (V) (4). Strait line is a line y = x showing that total arsenic concentration after 20 min of irradiation is equal to the starting p-ASA concentration. Insert – ratio of [As(III)]/[As(V)] after 20 min of irradiation at different initial concentrations of pASA. [Fe(III)] = 2×10-5 M, [Oxalate] = 1.2×10-4 M, [PS] = 10-3 M, accordingly.

Supplementary Files

This is a list of supplementary files associated with this preprint. Click to download.

- 2020pASAFeOX3PSESIV6.docx